PHILOSOPHICAL MAGAZINE B, 1999, VOL. 79, NO. 11/12, 2027–2035

Inelastic X-ray scattering determination of the dynamic structure factor of liquid lithium

T. SCOPIGNO†¶, U. BALUCANI‡, A. CUNSOLO§, C. MASCIOVECCHIO§, G. RUOCCO‖ and F. SETTE§

† Dipartimento di Fisica and Istituto Nazionale per la Fisica della Materia, Università di Trento, I-38050 Povo, Trento, Italy
‡ Istituto di Elettronica Quantistica, Consiglio Nazionale delle Ricerche, 50127 Firenze, Italy
§ European Synchrotron Radiation Facility, F-38043, Grenoble Cedex, France
‖ Dipartimento di Fisica and Istituto Nazionale per la Fisica della Materia, Università di L'Aquila, I-67100 L'Aquila, Italy

ABSTRACT

We present new inelastic X-ray scattering data for the dynamic structure factor $S(Q,\omega)$ of liquid lithium collected at two different temperatures ($T = 475\,K$ and $T = 600\,K$) and in a wide range of exchanged wave-vectors ($Q = 1\,nm^{-1}$ to $Q = 110\,nm^{-1}$). The analysed Q range covers the transition from collective to single-particle regimes. The spectra have been put on an absolute scale using its first sum rules, and the result obtained has been tested on diffraction data and novel molecular dynamic results. A relaxation fingerprint is observed at low wave-vectors (the so-called positive dispersion of the apparent sound speed), while at higher Q the single particle behaviour gradually emerges.

§ 1. INTRODUCTION

The structure and dynamics of molten metals embody the main features of simple liquids and for this reason interpreting their behaviour is of basic importance for understanding the interatomic interactions in condensed matter (Balucani and Zoppi 1994). In particular, the collective dynamics of such systems, unlike the Lennard-Jones fluids, shows well defined excitations extending well beyond the hydrodynamic region. Although the existence of collective motion has been clearly indicated by a large amount of experimental data, the available inelastic spectra often do not allow an accurate analysis and a cutting-edge investigation is a challenging task.

Up to few years ago the only experimental probe adequate for accessing such dynamics was neutrons. In this case the inelastic scattered intensity is given by

$$I(Q,\omega) = \frac{\sigma_c}{\sigma_c + \sigma_i} S(Q,w) + \frac{\sigma_i}{\sigma_c + \sigma_i} S_{self}(Q,\omega),$$

¶ Email: scopigno@science.unitn.it.

Philosophical Magazine B ISSN 0141–8637 print/ISSN 1463–6417 online © 1999 Taylor & Francis Ltd
http://www.tandf.co.uk/JNLS/phb.htm
http://www.taylorandfrancis.com/JNLS/phb.htm

where σ_c and σ_i indicate the coherent and incoherent parts respectively of the scattering cross-section. Therefore, aiming at the collective motion analysis, the first limit arises from the necessity of removing the single-particle contribution. Normally this is done by making an *Ansatz* for the self-contribution line shape, namely by introducing some additional parameters into the fitting procedure (De Jong 1993).

An even more serious drawback of inelastic neutron scattering (INS) is dictated by the fulfilment of kinematic restrictions; the conservation of the transferred momentum and energy, together with the neutron dispersion relation often confines the lower Q value accessible to INS quite outside the hydrodynamic region, say, beyond the first sharp diffraction peak (FSDP), the exact edge being settled by the velocity of neutrons and by the sound speed of the system (Lovesey 1984) (hot neutrons and heavy elements are preferred). Looking at alkali metals such limitations start to be effective below rubidium, the sound speed of potassium being around 2000 m s^{-1}.

For all these reasons inelastic X-ray scattering (IXS) is particularly advantageous for those light elements where the incoherent neutron cross-section is not negligible. Lithium is probably the best example, owing to the high sound speed (around 5000 m s^{-1}). In Li the neutron scattering cross-sections are comparable ($\sigma_i \approx 1.1\sigma_c$) and this poses further challenges to INS in this system (Verkerk *et al.* 1992, De Jong *et al.* 1993); on the other hand no incoherent contribution affects X-ray cross-sections in monoatomic systems. Moreover basically no restrictions occur concerning the accessible Q region, the only limitations being due to the necessity of resolving the scattered flux from the incoming beam at low Q values and from the decrease in form factor at high Q values. Finally constant-angle scans correspond to constant-Q scans, showing in a direct and clear way the dynamic response.

Since the first IXS experiments, lithium has been considered as the most favourable system, owing to its low atomic number (in an optimized experiment, i.e. low photoelectric absorption, the overall scattered signal for IXS is proportional to Z^{-2}), high sound speed (so that the inelastic contributions are well separated from the quasielastic contributions) and quite favourable inelastic-to-elastic ratio (Burkel 1991, Sinn *et al.* 1997)

In this work we report the results of a new series of IXS experiments performed at the beam line BL21 of the European Synchrotron Radiation Facility on liquid lithium at two different temperatures T = 475 K (slightly above the melting point) and T = 600 K. The availability of different scattering geometries allowed us to access an extremely wide range of exchanged wave-vectors from 1 to 110 nm^{-1}, so that it has been possible to follow entirely the transition from strongly correlated to single-particle dynamics. Owing to the high flux available and to the extremely high resolutions achieved recently (comparable with neutron experiments) we are now able to perform an accurate line-shape analysis of the collective dynamic response and consequently to establish the nature and features of the relaxation processes involved (Scopigno *et al.* 1999a). In particular a highly debated subject is the origin and behaviour of the so-called positive dispersion, a typical feature of simple liquids which is manifested as an increase in the effective sound speed at increasing wave-vector. In this work we investigate the behaviour of such dispersion at two different temperatures; a strong temperature dependence is expected to be the fingerprint of a thermally activated mechanism ruled by a relaxation time(s) which strongly decreases with increasing temperature.

§ 2. The experiment

2.1. *Experimental details*

The lithium sample was purchased from Goodfellows and the atomic masses are in the natural abundance ratio. The sample was heated in an austenitic stainless steel cell via the resistive method, the whole enviroment being kept in a standard vacuum set-up to prevent any oxidation.

The data were collected at constant Q in different configurations; below the FSDP and for both temperatures we used the horizontal scattering geometry, collecting the beam simultaneously with five different analysers. In this geometry we used two different resolutions: the Si(999) reflection from perfect silicon cristals ($\Delta E \approx 3$ meV) for most of the Q values, and the Si(11 11 11) ($\Delta E \approx 1.5$ meV) for the lower and upper edges (at low Q, $S(Q,\omega)$ becomes narrower so that a higher resolution is suitable while, at the maximum horizontal scattering angle, the higher energy used to match the Si(11 11 11) gives a higher Q value). Beyond the FSDP the spectra become broader so that we used the vertical scattering geometry, collecting the beam with a single analyser working at Si(777) ($\Delta E \approx 8$ meV) which can reach much larger angles (around 145°); this configuration was used only at $T = 475$ K. The wave-vector resolution is $\Delta Q \approx 0.2\,\mathrm{nm}^{-1}$ in the horizontal scattering configuration and $\Delta Q \approx 0.3\,\mathrm{nm}^{-1}$ in the vertical configuration. More details about BL21 have been published elsewhere (Masciovecchio *et al.* 1996a,b, Verbeni *et al.* 1996).

2.2. *Data reduction*

All the scans contributing to a single Q setting were added and then normalized to the monitor. We observed and subtracted a non-negligible empty cell scattering only in the range $8\,\mathrm{nm}^{-1} < Q < 13\,\mathrm{nm}^{-1}$, probably owing to scattering from the windows of the vacuum chamber occurring in that Q region.

The main problem usually encountered in IXS normalizations involves the absolute normalization of the spectra; the scattered intensity and the dynamic structure factor are in fact related by some quantity including the different efficiencies of the analysers and the atoms' form factor. To bypass such difficulties and because of the fully coherent IXS response, we adopted a very simple procedure based on the knowledge of the first frequency moments of the dynamic structure factor.

The first two frequency moments of $S(Q,\omega)$ are in fact

$$m_0^S = \int S(Q,\omega)\,\mathrm{d}\omega = S(Q),$$

$$m_1^S = \int \omega S(Q,\omega)\,\mathrm{d}\omega = \frac{\hbar Q^2}{2M}.$$

Let us denote by

$$I(Q,\omega) = \alpha \int R(\omega' - \omega) S(Q,\omega')\,\mathrm{d}\omega'$$

the measured intensity where $R(\omega)$ is the resolution function and α a constant including the form factor and efficiency. The frequency moments of S, I and R will be related by

$$m_0^I = \alpha m_0^R m_0^S,$$

$$m_1^I = \alpha (m_0^R m_1^S + m_1^R m_0^S),$$

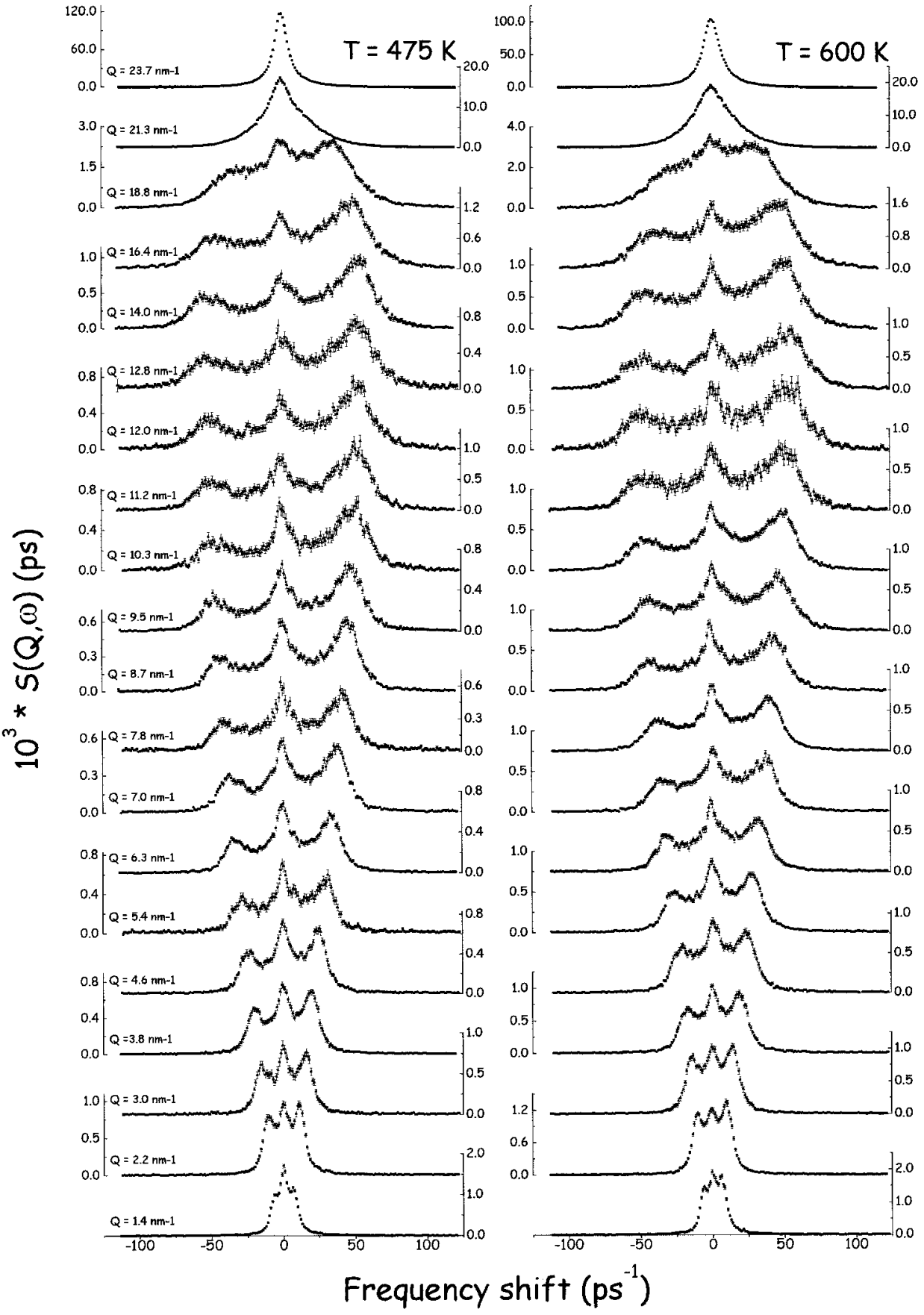

Figure 1. IXS spectra of liquid lithium at the two different temperatures. The reported data, normalized and corrected for the empty cell contributions, have been collected in the horizontal configuration with 3 meV of energy resolution (full width at half-maximum (FWHM)).

so that, once we calculate the first two frequency moments of the measured intensity and resolution, we get for the structure factor the relation

$$S(Q) = \frac{\hbar Q^2/2M}{m_1^I/m_0^I - m_1^R/m_0^R}.$$

This value can be used to normalize the scattered intensity to the spectrum $S(Q,\omega)$; it is worth noting that for symmetrical resolution functions ($m_1^R = 0$) the ratio of the first two frequency moments of intensity and $S(Q,\omega)$ exactly coincide.

We adopted the above procedure to normalize all the spectra (shown in figures 1 and 2, where we report the spectra in the horizontal and vertical scattering geometries respectively) and compared the obtained structure factor with experimental (X-ray and neutron diffraction (Sjölander 1987)) and computer simulation data (Scopigno *et al.* 1999b); in the latter case the result for the $T = 475$ K set is reported in figure 3.

§ 3. Discussion

The quantity that in a simple liquid is closer to the speed of sound of a solid system is the maximum of the current correlation function

$$J(Q,\omega) = \frac{\omega^2}{Q^2} S(Q,\omega).$$

In fact, assuming that the density correlator (whose Fourier transform is $S(Q,\omega)$) obeys a generalized Langevin equation characterized by a memory function decaying over a certain time scale τ, it can be shown how the maximum of $J(Q,\omega)$, say, ω_m, undergoes a cross-over from a viscous to elastic response when the condition $\omega\tau = 1$ holds. In particular, in the high-frequency limit the value of ω_m/Q approaches the so-called instantaneous sound speed c_∞; the liquid shows a solid-like response and the parameter embodying such behaviour is just the current correlation maximum.

In figure 4 we report $\omega_m(Q)$ as a function of the momentum transfer (figure 4(*a*) shows the full data while figure 4(*b*) emphasizes the low-Q region). The value of the sound speed extrapolated at small Q from the dispersion curve, calculated from neutron scattering or computer simulation, is always compared with the adiabatic speed of sound, *but that is not generally correct* and the case of lithium is a clear example. In fact, in all the non-conductive simple or complex fluids (rare gas, water or glass formers) the relatively low thermal diffusivity D_T makes the thermal relaxation time $\tau_T = 1/\gamma D_T Q^2$ so long as the transition from the adiabatic ($\omega\tau_T \gg 1$) to isothermal ($\omega\tau_T \ll 1$) regime effectively occurs outside the hydrodynamic region. A totally different scenario characterizes instead conductive liquids; in this case the much larger thermal diffusivity (Cook and Fritsch 1985) causes shortening of the relaxation time so that the transition occurs at quite low Q values. In the case of lithium the condition $\omega\tau_T = 1$ is met at about $Q = 0.2\,\mathrm{nm}^{-1}$ so that in the IXS window the 'small-Q' limit means the isothermal and not the adiabatic limit. For this reason it is more meaningful to compare our experimental data with the isothermal dispersion relation. In practice in lithium the difference between the isothermal and adiabatic sound speed is only 3% because the specific heat ratio $\gamma \approx 1$.

At higher wave-vectors the bending down of the dispersion curve associated with structural effect (the increase in the structure factor) is preceded by a wave-vector range where another relaxation mechanism (usually referred to as shear relaxation) is

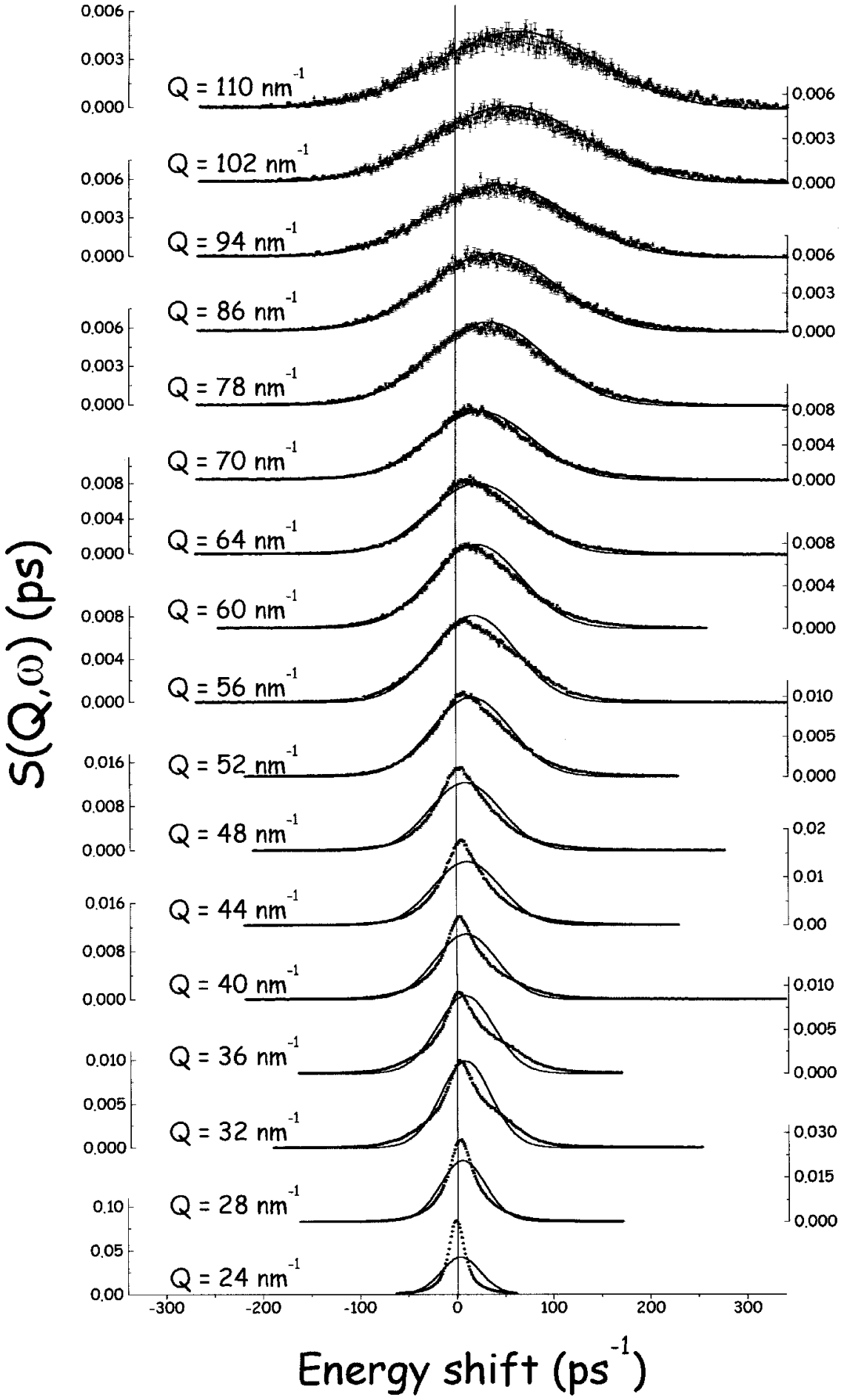

Figure 2. Same as figure 1 but at a higher Q value in the vertical scattering configuration (energy resolution of 8 meV). The free-particle limit is reported at each Q value as a comparison.

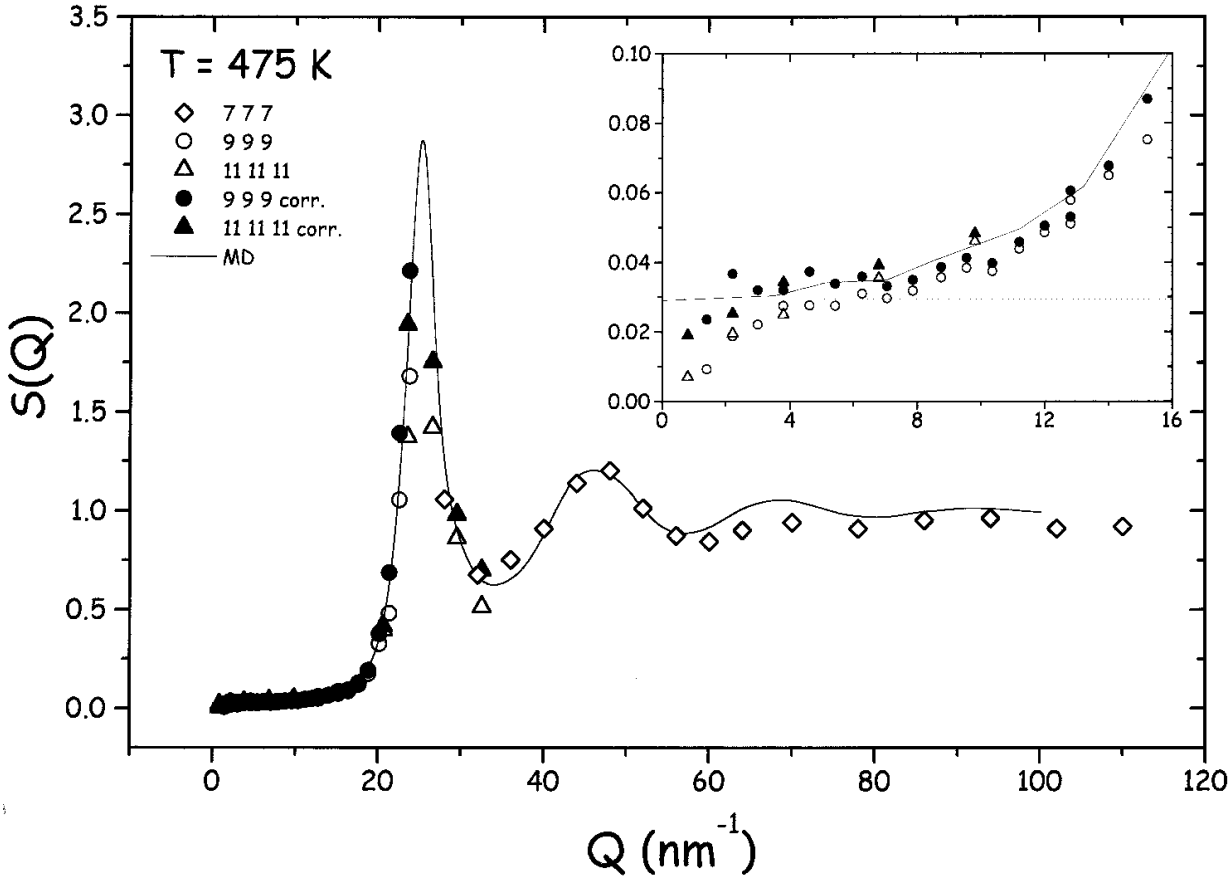

Figure 3. Structure factor at $T = 475$ K as calculated from experimental data with the procedure discussed in the text. At low Q we report both the results obtained by taking into account the resolution asymmetry effects and by ignoring them. In the lower-resolution configuration no significant differences were observed. The experimental results are compared with data from molecular dynamics simulation (Scopigno *et al.* 1999b).

effective. This process causes a sudden increase in the sound speed of the order of 25%. The temperature dependence of such mechanism appears to be quite modest; on increasing the temperature the transition moves to slightly higher Q values, consistent with a decrease in the relaxation time. In any case the explored temperature range seems to be too limited to draw any definite conclusion from the raw experimental data without making any models for the memory function details and for the number of the involved relaxation mechanisms (Scopigno *et al.* 1999a).

At even larger wave-vectors, the current maximum $\omega_m(Q)$ starts to approach the free-particle limit. The latter is easily calculated as the maximum of the function

$$J_{free}(Q,\omega) = \frac{\omega^2}{Q^2}\frac{S(Q)}{\sqrt{(2\pi)^{1/2}}}\left(C^{(7)}\frac{\exp[-(\omega-\omega_0^{(7)})^2/2\sigma^{(7)2}]}{\sigma^{(7)}} + C^{(6)}\frac{\exp[-(\omega-\omega_0^{(6)})^2/2\sigma^{(6)2}]}{\sigma^{(6)}}\right)$$

with

$$\omega_0^{(i)} = \frac{\hbar Q^2}{2M_i}, \quad \sigma^{(i)2} = \frac{KT}{M_i}Q^2$$

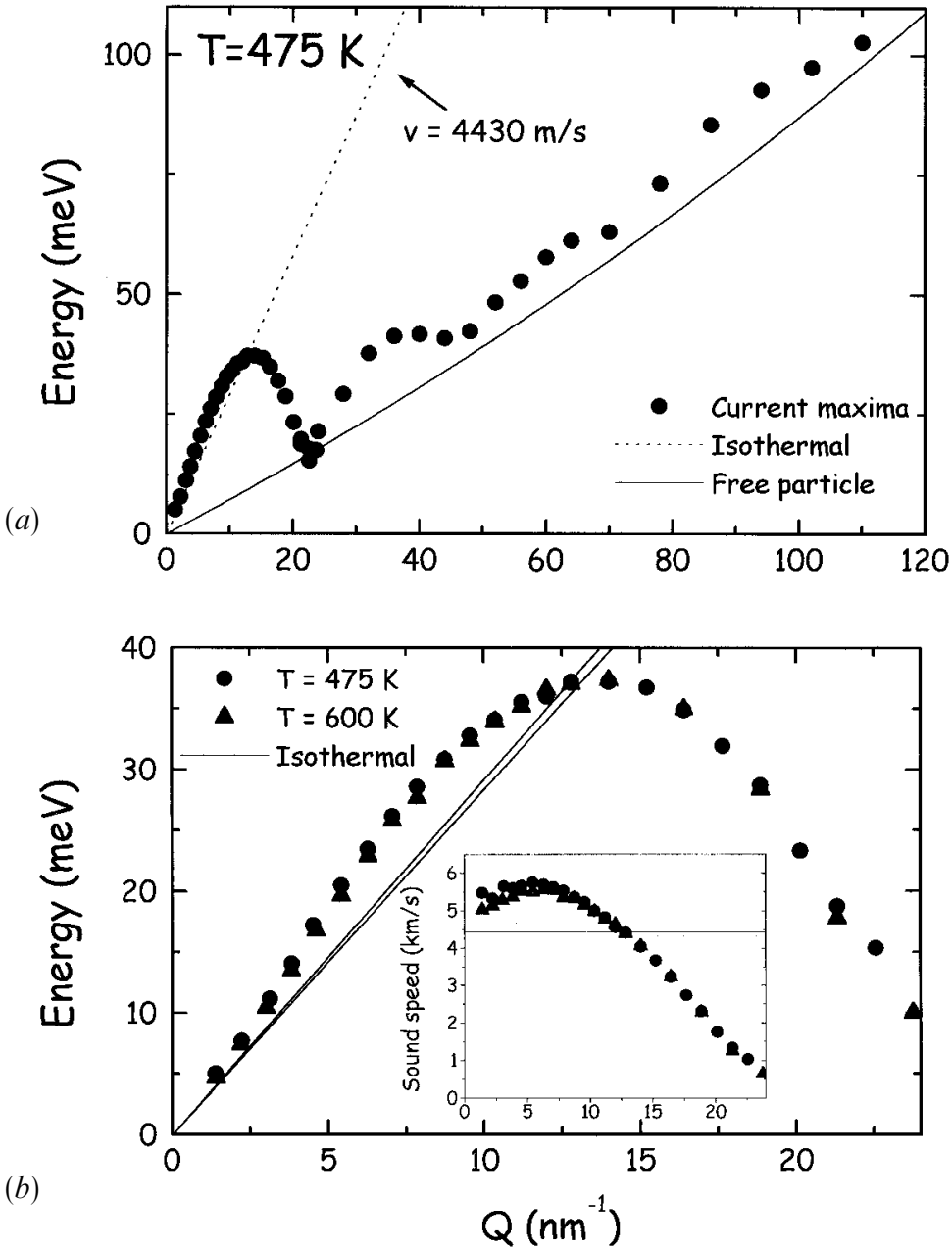

Figure 4. (*a*) Longitudinal current correlation maxima at $T = 475$ K in the full dynamic region accessed. The limiting isothermal and free-particle sound velocities are also reported. (*b*) Same as (*a*) but at two different temperatures and in the small-Q region (resolutions of 1.5 and 3.0 meV FWHM). The positive dispersion before the structural bending down appears clearly in the inset.

where C indicates the isotopic concentration ($C^{(6)} = 0.08$ and $C^{(7)} = 0.92$ for ^{6}Li and ^{7}Li respectively). For a single isotope system we can easily obtain

$$\omega_{m,free}(Q) = \frac{\omega_0 \pm (\omega_0^2 + 8\sigma^2)^{1/2}}{2},$$

where the two solutions are due to the quantum behaviour of $S(Q,\omega)$. The general case of different isotopic species has no analytical solution; so the two solutions must be evaluated numerically. In figure 4 we report the theoretical values for the anti-Stokes side.

The approach to the self-dynamics is clearly shown in figure 2 where we report the experimental $S(Q,\omega)$ above the FSDP superimposed on the Gaussian model and

from figure 4 where the current maxima are shown together with the isothermal (hydrodynamic limit) sound speed and with the value calculated from the above expression (free-particle limit) representing the opposite approximations (low and high Q) bounding the true sound speed behaviour.

The ω_m values wiggle as a function of the exchanged wave-vector with a phase opposite to the S(Q) phase as expected in the case of vibrational dynamics of solids, with the minima of such oscillations approaching the free-particle limit with increasing wave-vector.

References

Balucani, U., and Zoppi, M., 1994, *Dynamics of the Liquid State* (Oxford: Clarendon).

Burkel, E., 1991, *Inelastic Scattering of X-rays with Very High Energy Resolution* (Berlin: Springer).

Cook, J. G., and Fritsch, G. H., 1985, *Handbook of Thermodynamic and Transport Properties of Alkali Metals* edited by R. W. Oshe (Oxford: Blackwell Scientific), p. 735.

De Jong, P. H. K., 1993, PhD Thesis, Technische Universiteit Delft, The Netherlands.

De Jong, P. H. K., Verkerk, P., and De Graaf, L. A., 1993, *J. non-crystalline Solids*, **156–158**, 48.

Lovesey, S. W., 1994, *Theory of Neutron Scattering from Condensed Matter* (Oxford: Clarendon), p. 120.

Masciovecchio, C., Bergman, U., Krish, M., Ruocco, G., Sette, F., Verbeni, R., 1996a, *Nucl. Instrum. Meth.* B, **111**, 181; 1996b, *ibid.*, **117**, 339.

Scopigno, T., Balucani, U., Ruocco, G., and Sette, F., 1999a (to be published); 1999b (to be published).

Sinn, H., Sette, F., Bergmann, U., Halcoussis, C., Krish, M., Verbeni, R., and Burkel, E., 1997, *Phys. Rev. Lett.*, **78**, 1715.

Sjölander, A., 1987, *Amorphous and Liquid Materials* edited by E. Lüscher, G. Fritsch and G. Jacucci (Dordrecht: Martinus Nijhoff), p. 239.

Verbeni, R., Sette, F., Krish, M., Bergman, U., Gorges, B., Halcoussis, C., Martel, K., Masciovecchio, C., Ribois, J. F., Ruocco, G., and Sinn, H., 1996, *J. Synchrotron Radiat.*, **3**, 62.

Verkerk, P., de Jong, P. H. K., Arai, M., Bennington, S. M., Howells, W. S., and Taylor, A. D., 1992, *Physica* B, **180 & 181**, 834.